Journal of Flood Risk Management

WILEY

CIWEM Chartered Institution of Water and Environmental Management | Journal of Flood Risk Management

ORIGINAL ARTICLE OPEN ACCESS

Assessing Causes and Consequences of Winter Surface Water Dynamics in California's Central Valley Using Satellite Remote Sensing

Christine M. Albano[1] | Christopher E. Soulard[2] | Blake A. Minor[1] | Jessica J. Walker[3] | Britt W. Smith[3] | Eric K. Waller[4] | Michael D. Bartles[5] | Thomas W. Corringham[6] | Anthony T. O'Geen[7] | Melissa M. Rohde[8,9] | Anne M. Wein[2]

[1]Desert Research Institute, Division of Hydrologic Sciences, Reno, Nevada, USA | [2]US Geological Survey, Western Geographic Science Center, California, USA | [3]US Geological Survey, Western Geographic Science Center, Tucson, Arizona, USA | [4]US Geological Survey, Geosciences and Environmental Change Science Center, Denver, Colorado, USA | [5]Hydrologic Engineering Center, US Army Corps of Engineers, Davis, California, USA | [6]Scripps Institution of Oceanography, University of California San Diego, La Jolla, California, USA | [7]Department of Land, Air and Water Resources, University of California, Davis, California, USA | [8]Rohde Environmental Consulting LLC, Seattle, Washington, USA | [9]SUNY College of Environmental Science and Forestry, Syracuse, New York, USA

Correspondence: Christine M. Albano (christine.albano@dri.edu)

Received: 26 December 2024 | **Revised:** 22 April 2025 | **Accepted:** 14 May 2025

Funding: Funding for this work was provided by the US Geological Survey through grant agreement number G21AC10098 and the US Army Corps of Engineers, Engineer Research and Development Center through grant agreement number W912HZ1920011.

Keywords: dynamic surface water extent | flood | groundwater recharge | moderate resolution imaging spectroradiometer (MODIS)

ABSTRACT

California's Central Valley is increasingly vulnerable to winter floods. A comprehensive spatial baseline of flood extents is critical for inundation analyses that can enhance future flood predictions, but cloud cover has prevented the regular observation of surface water extents with optical satellite imagery. In this study, we leveraged the daily resolution of Moderate Resolution Imaging Spectroradiometer (MODIS) satellite data to create a continuous series of monthly Dynamic Surface Water Extent (DSWEmod) images across the Central Valley from January 2003 to January 2023. We used the timeseries to assess the climatic driving forces of winter (Oct–April) surface water variability at sub-basin and pixel scales. At the sub-basin scale, we evaluated the influences of winter precipitation, occurrence of atmospheric rivers, and antecedent soil moisture on monthly surface water extents and found that the greatest correspondence occurs in mid-winter (Dec–Feb); in contrast, non-precipitation drivers such as water management play a stronger role in autumn and spring. The pixel-level analysis identified the probabilities of precipitation-driven surface water occurrences in the Sacramento basin are highest along rivers, conveyance channels, and floodways, with higher probabilities under wetter antecedent soil moisture conditions. Precipitation-driven surface water occurrences are also common in leveed areas and outside flood boundaries designated by state and federal agencies where exposure of structures to inundation was larger in terms of their value. Finally, areas with more frequent precipitation-driven flooding have poor recharge potential but are commonly within 5 km of areas classified as having good potential. This study demonstrates a novel approach for exploring the utility of MODIS for understanding surface water dynamics in mid-winter, a period characterized by peak precipitation, flood risk, and surface water extent. This information can provide valuable insights for (1) assessing flood risks for infrastructure and populations, (2) identifying areas most suited to strategic water management investments to increase recharge, and (3) analyzing precipitation thresholds that trigger flooding to allow proactive water management strategies to minimize damage and maximize recharge.

1 | Introduction

Characterization and prediction of flood inundation are critical science needs for emergency response, flood hazard, and water management planning. Satellite-based monitoring of surface water extents for this purpose has been conducted for several years through programs such as the NASA Global Flood Mapping System (Policelli et al. 2017), but the ability to readily process and analyze entire collections of imagery to characterize spatial and temporal patterns of surface water dynamics in relation to weather phenomena has only recently become possible (e.g., Jones 2019; Pekel et al. 2016), expedited in part through the use of cloud computing platforms like Google Earth Engine (Gorelick et al. 2017).

In the Central Valley of California (Figure 1), over 1.3 million people, $223 billion in structures, and $17 billion in agricultural economic activity are increasingly exposed to flood risks due to climate change and aging infrastructure (California Department of Water Resources 2022), population growth and agricultural land use intensification (Reiter et al. 2015), and land subsidence resulting from groundwater extraction (Faunt et al. 2016). In this region, flooding occurs primarily in association with wintertime precipitation caused by atmospheric rivers (ARs). ARs

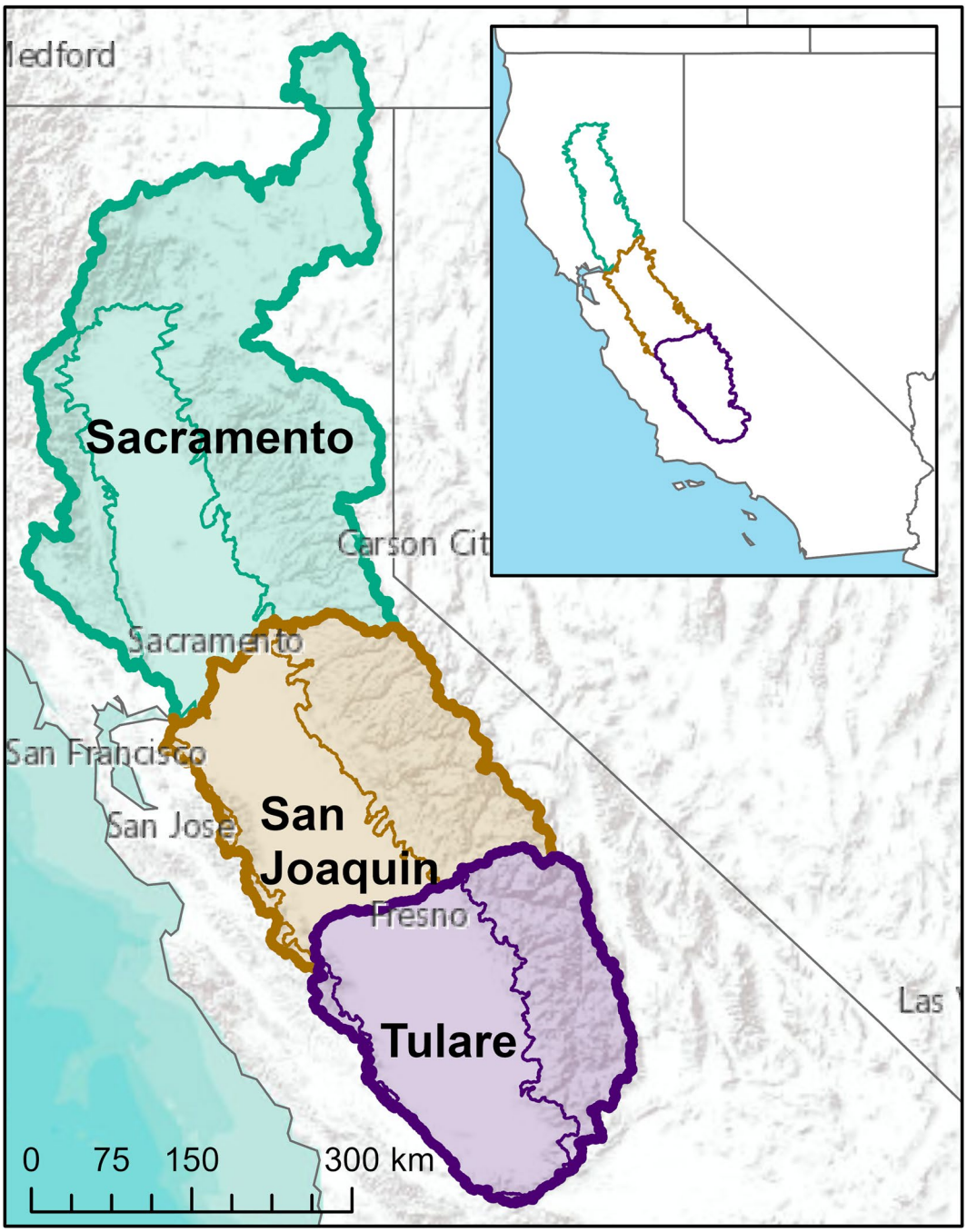

FIGURE 1 | Study area, including the alluvial portions of the Central Valley (thin lines) where surface water extents were analyzed, and Sacramento, San Joaquin, and Tulare (HUC-4) contributing areas (heavier lines) within which monthly precipitation and antecedent soil moisture values were averaged.

are long corridors of water vapor transport that extend from the tropics to mid-latitudes (Zhu and Newell 1998). When they reach the coastline of California and other regions around the world, the water vapor is uplifted by the terrain, it cools and condenses, and can result in heavy precipitation (Ralph et al. 2020). Although ARs do not account for all precipitation in the region, they are responsible for the largest magnitude floods (Dettinger et al. 2019) and more than 95% of flood damage costs between 1978 and 2017 across the state (Corringham et al. 2019). Late winter and springtime flooding can also occur and is common in the higher elevation catchments of the Tulare and San Joaquin basins, where more precipitation is stored as snowpack (Lund 2012).

A set of "Best Available Maps" that identify potential flood risks in the Central Valley is maintained and updated regularly by the California Department of Water Resources (DWR) (http://gis.bam.water.ca.gov/bam/). These maps were developed through engineering studies by the Federal Emergency Management Agency (FEMA), US Army Corps of Engineers (USACE), and DWR for different purposes; however, these maps do not necessarily represent specific events or storm patterns in the historical record (Tellman et al. 2021). Long-term records of streamflow observations are an important indicator of flood conditions (Walker et al. 2020) but do not comprehensively capture spatial patterns relating to flood depth, duration, and extents, which have greater direct relevance and impacts upon species habitat, residential communities, and infrastructure outside of stream channels. Moreover, as interest in utilizing flood waters for aquifer recharge increases (Charles 2023; Kocis and Dahlke 2017; Reddy et al. 2017), more knowledge of the spatial distributions of flood waters during wintertime is needed, but long-term data quantifying this are lacking.

Several satellite-based data products have been used for surface water extent and flood monitoring (Policelli et al. 2017), including optical reflectance products from Landsat and Moderate Resolution Imaging Spectroradiometer (MODIS), which have been in operation since the years 1972 and 2000, respectively. While the Landsat satellite is unparalleled in terms of its lengthy historical record and moderate spatial resolution (30-m), its low frequency of observations (~every 16 days) and inability to detect ground conditions in the presence of cloud cover limit its application to assess immediate and short duration changes in flood extents in association with precipitation events. This limitation has been identified in several past studies (Heimhuber et al. 2017; Vuolo et al. 2017; Wulder et al. 2016) and more recently in Walker et al. (2020), which showed that Landsat's ability to detect surface water dynamics during wintertime in California is limited due to a lack of cloud-free images. In contrast to Landsat, the daily observation frequency of MODIS products greatly increases the odds of capturing changes in surface water extent caused by precipitation events (Policelli et al. 2017), albeit at coarser spatial resolution (at least 250 m) and with a shorter historical record (2000–2023).

The Dynamic Surface Water Extent (DSWE) model was originally developed to identify and categorize occurrences of surface water using 30-m Landsat imagery. DSWE uses a composite score approach based on spectral and terrain characteristics to classify pixels according to the likelihood of water or wetland presence (Jones 2019). The desire to investigate winter water dynamics in California led to the adaptation of the DSWE algorithm to map inundation across the MODIS archive based on the hypothesis that the daily frequency of MODIS imagery could enable the creation of cloud-free maps by compositing images collected over multiple days. This method, referred to as DSWEmod, led to composite interval products of 5, 10, 15, and 30 days (monthly) for 2003 through 2019 (Soulard et al. 2021, 2022). Results for California show that monthly DSWEmod maps average 0.4% cloud obstruction during summer months and increase nominally to 1.4% in winter months. The cloud-free DSWEmod product was found to have high overall surface water mapping accuracy in California (>92%) in an assessment of the high confidence water class (HCW) in summer months (Soulard et al. 2022). Here, we extend the application of DSWEmod to identify its utility in increasing understanding of the causes and consequences of precipitation-driven surface water dynamics.

The objective of this study is to characterize the relationship of MODIS-derived winter surface water dynamics in the Central Valley of California with (1) weather patterns, including atmospheric river landfalls and precipitation, and (2) antecedent soil moisture conditions, which influence storm runoff and flooding effects in this region (Cao et al. 2020; Ralph et al. 2013; Sumargo et al. 2021). The study area includes the three large river basins (hydrologic unit code [HUC] 4; US Geological Survey 2019); Sacramento, San Joaquin, and Tulare-Buena Vista Lakes basins (the latter is hereafter referred to as Tulare) that comprise the Central Valley (Figure 1). First, we assess monthly variability in the areal extent of surface water within the alluvial portions of each river basin in relation to AR landfalls along the coastline as well as precipitation totals and antecedent soil moisture conditions within each basin's contributing area. Second, we identify specific locations where surface water appearances have statistically significant relationships to basin precipitation. We then use these relationships to estimate probabilities of surface water appearances over a range of precipitation and antecedent soil moisture conditions. Third, we overlay our results with natural and human-built infrastructure datasets as well as National Flood Insurance Program (NFIP) claims data to assess flood exposure and floodwater management potential across the Central Valley of California study area. To our knowledge, this is the first study to use remote sensing to examine mid-winter surface water dynamics in this region. Previous research omitted these months, presumably due to a lack of cloud-free imagery (Reiter et al. 2015; Schaffer-Smith et al. 2017). Our study thus provides a new perspective on the location, frequency, and extent of surface water inundation during wintertime flood events in the study area and has direct relevance to flood water management planning.

2 | Data and Methods

2.1 | Dynamic Surface Water Extent—MODIS (DSWEmod)

The DSWE model uses spectral and terrain characteristics to classify downscaled 250-m pixels according to water and wetland confidence: "high confidence water" (class 1), "moderate

confidence water" (class 2), "partial surface water-conservative" (class 3), "partial surface water-aggressive" (class 4), and "not water" (class 0). (Jones 2019). In a California study using MODIS imagery to create DSWE products, Soulard et al. (2022) reported that "high confidence" water pixels were the most reliable indicators of surface water, and the lower confidence water classes (classes 3 and 4) included considerably more errors, such as spectral confusion with urban areas. These errors, along with similar findings in other DSWE investigations (Vanderhoof et al. 2020) informed our decisions to primarily focus on "high confidence" water pixels (hereafter, HCW; class 1) for our analyses. In this study, monthly DSWE MODIS (DSWEmod) composites for Jan 2003–Jan 2023 were used because the monthly product provides the most continuous record (i.e., very little cloud obstruction). The compositing method prioritizes higher confidence DSWEmod classes over lower classes to maximize capture of HCW occurring during the composite period (Soulard et al. 2022). Monthly DSWEmod and Landsat DSWE composites are available for viewing at https://dri-apps.projects.earthengine.app/view/dswe.

2.2 | Meteorological Data

We used the daily, 1-km resolution Western Land Data Assimilation System dataset (WLDAS; Erlingis et al. 2021) to characterize monthly precipitation and antecedent soil moisture. This dataset was selected because of its high spatial resolution and inclusion of soil moisture and snow variables that could be used to characterize antecedent conditions. Monthly sums of precipitation (Rainf_f_tavg) were calculated for each pixel and then the spatial average of all pixels in each HUC-4 contributing area (refer to Figure 1) was calculated for each month. To calculate antecedent soil moisture, the volumetric soil moisture values for the top three soil layers (0–10, 10–40, 40–100 cm) were averaged for the first day of each month. Antecedent soil moisture values were spatially averaged across the same HUC-4 extents, filtered to include late autumn, winter, and early spring months (October to April) in 2003–2023, and binned into three quantile groups representing dry, moderate, and wet antecedent soil moisture within each HUC. AR landfall occurrences along the California coastline (30°–45° latitude) during the study period were drawn from an existing catalog of events (Gershunov et al. 2017). ARs were classified on a scale of 1 (weak) to 5 (exceptional) using the Ralph et al. (2019) scaling system following methods described in (Corringham et al. 2019).

2.3 | Infrastructure and Flood Boundaries Data

We obtained flood boundaries and infrastructure data from the Best Available Maps database (https://gis.bam.water.ca.gov/bam/; accessed June 15, 2022). Flood boundary datasets include DWR Flood Awareness, Regional Studies, USACE comprehensive studies, and FEMA Digital Flood Insurance Rate Maps (DFIRM). Flood infrastructure datasets include conveyance channels and designated floodways. Leveed areas (i.e., the area of a floodplain from which flood water is excluded by the levee system) were downloaded from the National Levee Database (https://levees.sec.usace.army.mil/; accessed June 15, 2022). Non-flood control infrastructure included buildings from the National Structure Inventory dataset (US Army Corps of Engineers 2019). Finally, we included a natural infrastructure dataset, the Soil Agricultural Groundwater Banking Index (SAGBI; O'Geen et al. 2015), in the analysis to identify opportunities for managed aquifer recharge. The SAGBI provides estimates of groundwater recharge suitability based on soil characteristics under natural (Unmodified) and under theoretical conditions of restrictive layers having been deeply tilled (Modified).

National Flood Insurance Program claims data (Federal Emergency Management Agency 2024) were compiled for the period of record, following Corringham and Cayan (2019). Each 0.1° pixel in this dataset was assigned 100-year, 500-year, or minimal flood hazard frequency based on the flood boundary type that covered the most area in the pixel. To accomplish this, flood boundary datasets were merged to delineate 100- and 500-year extents based on all data sources (FEMA DFIRM, USACE, and DWR Flood Awareness and Regional Studies), with the highest frequency flood risk taking priority in cases where datasets overlapped but had different flood risk designations. Thus, 100-year boundaries (FEMA DFIRM categories A, AE, A99, AH, AO) were given first priority, 500-year boundaries were given next priority, and all other areas designated as minimal flood hazard based on FEMA DFIRM were given third priority. The merged datasets representing minimal, 100-year, and 500-year flood boundaries were converted to raster datasets with 0.001° pixel resolution (approximately 100-m) to maintain their spatial precision and were then overlaid with the claims data to determine the flood hazard category that covered the most area in the pixel.

3 | Analytical Approach

We assessed relationships between surface water extents extracted from monthly DSWEmod composites (October–April) and monthly precipitation variability for the Jan 2003–Jan 2023 study period at two spatial scales to (1) determine how surface water extents change over time in relation to monthly weather (basin scale), and (2) identify locations where surface water appearances correspond with monthly weather (pixel scale). We then used results from the pixel-scale analysis to characterize how occurrence probabilities of surface water appearances correspond with natural and built infrastructure.

At the basin scale, we quantified the areal extents of HCW pixels within the alluvial portions of the Sacramento, San Joaquin, and Tulare basins of the Central Valley in each DSWEmod monthly composite. We then quantified linear relationships between surface water areal extents, AR landfalls along the California coastline, and spatially averaged precipitation and antecedent soil moisture metrics within each basin's contributing area (Figure 1; Albano et al. 2025).

For the pixel-scale analysis, we focused on identifying specific locations where the occurrence of surface water corresponded with increased monthly precipitation or soil moisture conditions. Instead of simply looking for the presence of HCW, we used a first-differencing approach to remove temporal autocorrelation (Wooldridge 2012) and instead analyze transitions from

no- or low-confidence water to moderate- or high-confidence water in the monthly data using logistic regression analysis. We defined a valid monthly transition as a minimum of two class changes between the lower and higher confidence water classes to reduce the likelihood of including spurious transitions caused by subtle spectral changes or shifts in pixel sample area. Thus, our binary response variable was defined as 1, which represents water appearance (i.e., minimum 2-step transition to a higher confidence class) and 0, which represents either water disappearance (i.e., transition from a higher confidence water class to a lower, partial, or not water class) or the persistence of partial or not water classes. In cases where high or moderate confidence water persisted, NA values were assigned, given the inability to determine the role of monthly climate on transitions between those classes.

We implemented a mixed effects model using the lme4 package (Bates et al. 2015; glmer function, family = binomial, bobyqa control optimizer) in R (R Core Team 2024) to estimate the probability of a given pixel transitioning to water, based on monthly basin-averaged precipitation totals (fixed effect; cube-root transformed to meet normality assumptions) and antecedent soil moisture (random effect with fixed intercept). We excluded pixels with a high number ($n > 100$) of no data values over the duration of the study period in the monthly DSWEmod composites. Model goodness of fit was assessed using the Performance package in R (Lüdecke et al. 2021) based on Tjur's coefficient of discrimination (Tjur 2009), which is a pseudo-R squared value recommended for use with mixed effects logistic regression.

We estimated predicted probabilities and associated confidence intervals (80%; $p < 0.1$) under low, moderate, and wet antecedent conditions for six values of average monthly precipitation (250–500 mm in increments of 50 mm) in each basin using the predictInterval function of the merTools package (Knowles and Frederick 2020). These precipitation amounts were selected to span the range of the largest total monthly precipitation amounts observed across the three basins during the WLDAS period of record (1980—2023; see Figure S1). Finally, we masked the pixel scale results to omit pixels with statistically non-significant ($p \geq 0.10$) relationships with monthly precipitation and applied a 3×3 cell moving window analysis, where focal cells within windows containing fewer than four statistically significant pixels were masked. This threshold was chosen to eliminate isolated pixels and focus on places with larger surface water extents. Based on a sensitivity analysis, this threshold results in a conservative estimate of the areal extent of flood exposure (refer to Supporting Information (SI) Figure S2). To characterize spatial patterns of precipitation-driven surface water occurrences, the filtered predicted probability and confidence interval maps were summarized in relation to flood infrastructure and zoning data.

To assess exposure of infrastructure, the predicted surface water appearance probabilities were overlaid on the National Structure Inventory dataset (US Army Corps of Engineers 2019) and roads (US Census Bureau 2022). Building exposure was measured by the values of the structures in the surface water pixels, although it is possible that the structures were not in an inundation area within the pixel. Values of exposed residential structures were overlaid by and compared to National Flood Insurance Program claims data across different flood hazard zones. Exposure estimation and results for roads are provided in the Supporting Information (refer to Figure S5). Predicted surface water appearance probabilities were also overlaid on the Soil Agricultural Groundwater Banking Index dataset to assess correspondence with estimates of groundwater recharge suitability. Recharge suitability considers the relative permeability of soils to promote recharge and the likelihood of prolonged root zone saturation, which can damage certain crops (O'Geen et al. 2015).

4 | Results

4.1 | Basin Scale Analysis of Surface Water Extents

The areal extents of DSWEmod HCW pixels (i.e., surface water extents) within the alluvial portions of the Sacramento, San Joaquin, and Tulare basins (Figure 1) exhibit seasonal patterns with increases in late autumn, peaks in winter, and decreases in early spring, although these patterns differ among basins in both timing and extent (Figure 2). The broadest extents occur in the Sacramento River portion of the Central Valley, where peaks typically occur in January and range between 1800 and 4000 km^2. In the San Joaquin and Tulare basins, peaks in the areal extent occur in January or February and cover substantially less area than in the Sacramento basin both proportionally and in absolute numbers. The largest surface water extents occur during the highest precipitation water years (water year defined as October–September), especially when monthly precipitation during November–January is higher than average (e.g., 2006, 2011, 2017, 2023). Large monthly precipitation amounts during February–April tend to sustain surface water extents over longer periods of time, rather than increase their area (Figure 2).

Although changes in monthly surface water extents exhibit correspondence with monthly precipitation amounts (Figure 2), the variation explained differs among basins and among late autumn, winter, and early spring months (Figure 3). Considering both monthly precipitation and antecedent soil moisture conditions, the Sacramento basin exhibits the largest absolute changes in surface water extents in relation to precipitation variability, and the Tulare exhibits the least. Although increases in surface water extents consistently occur in the autumn months in the San Joaquin and Sacramento basins (Figure 2), the strength of the relationship with monthly precipitation is relatively weak under dry soil moisture conditions, which occur most of the time, but is stronger under less-frequent, moderate soil moisture conditions. Overall, the relationships between monthly precipitation and changes in water are strongest (as indicated by steeper regression slopes) in mid-winter (December–February), and with wet antecedent soil moisture (Figure 3).

Across all basins, monthly atmospheric river (AR) statistics such as the maximum rank based on the Ralph et al. (2019) AR scale had weaker explanatory power than basin-precipitation estimates, and positive relationships were only observed in mid-winter (Dec–Feb; Figure 4). During this period, months with maximum AR ranks of 2 or greater resulted in increases in surface water extents, with the largest median increases occurring during months when Rank 4 ARs occurred. Despite the weak correspondence between AR rank and surface water extent, our

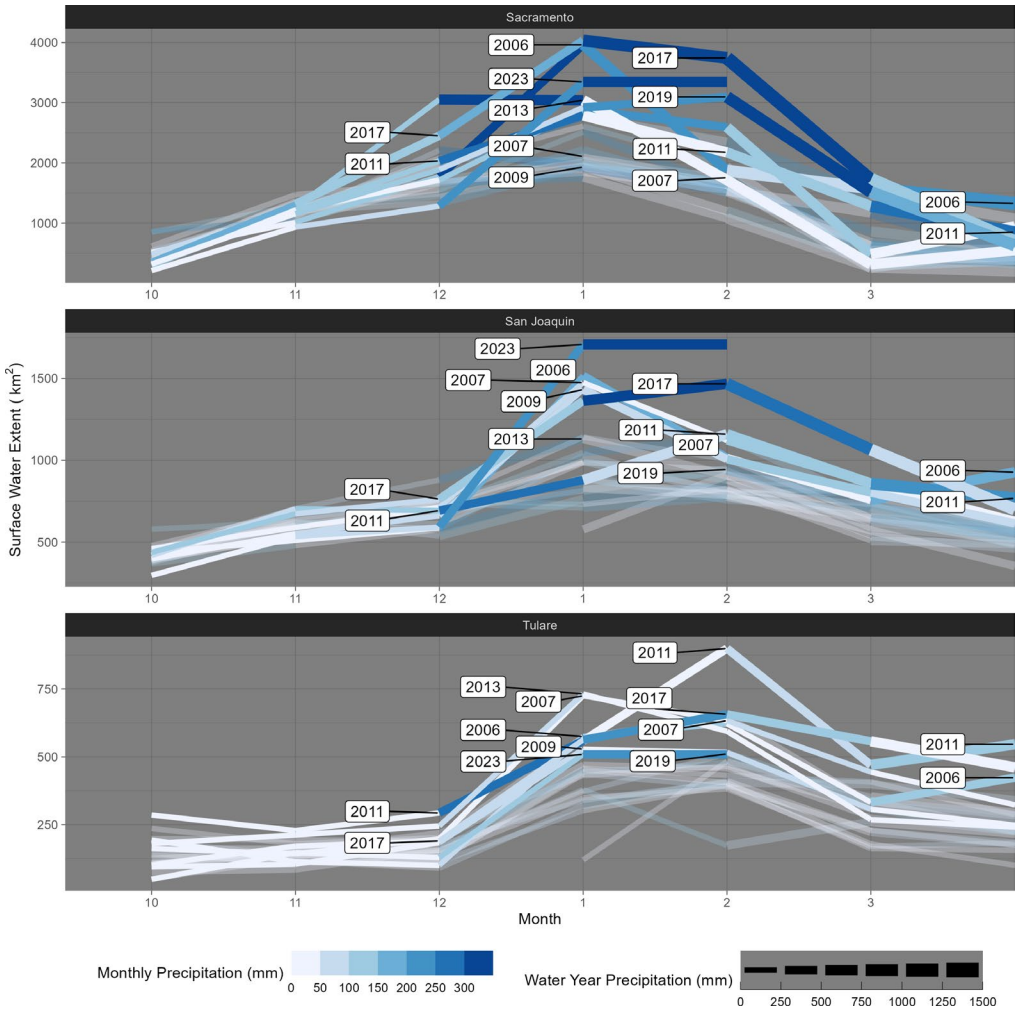

FIGURE 2 | Annual timeseries of surface water extents Jan 2003–Jan 2023. Line segments colored according to monthly precipitation amounts, line thickness represents cumulative water year precipitation. Years with largest changes are highlighted and labeled (other years are muted color).

results highlight the importance of ARs as determinants of winter water availability. For example, all winter months lacking an AR of rank 2 or greater resulted in reductions in surface water extents relative to previous months.

4.2 | Pixel Scale Analysis of Surface Water Appearances in Relation to Precipitation Variability

We conducted a pixel-scale analysis to explicitly identify where surface water appearances are related to precipitation within each basin. This spatial precision was intended to distinguish areas that are potentially most exposed to winter floods, as well as those areas where precipitation-dependent water management decisions drive surface water presence. Predicted probabilities of surface water appearance are most prominent in the lower Sacramento basin, where probabilities increase with increases in both precipitation and antecedent soil moisture (Figure 5). The effects of antecedent soil moisture exhibit greater influence in conveyance channels and floodways, where upstream water is routed, relative to leveed areas (Figures 5 and 6). Model-based uncertainties in the probability of surface water appearance for a given precipitation amount and soil moisture status vary widely, indicating considerable uncertainty in the model predictions. Uncertainty (as indicated by upper and lower confidence intervals) also increases with precipitation amounts; for example, the average (across soil moisture statuses) proportion of leveed areas in the Sacramento with greater than 60% probability of surface water appearance is between 0% and 6% (3–526 km^2) at 250 mm monthly precipitation but the uncertainty range essentially doubles to 1%–14% (72–1109 km^2) in the case of 500 mm precipitation (Figure 6). The ranges of areas with greater than 60% probability of surface water appearance across antecedent soil moistures vary with infrastructure type, with minimal difference between dry and wet conditions in leveed areas, 10% differences between dry and wet conditions in conveyance channels across all monthly precipitation amounts, and a slight increase in differences in floodways (going from 0% to 2%) with increasing precipitation (Figure 6).

4.3 | Structural Exposure to Precipitation-Driven Surface Water Appearances

As discussed in a DSWEmod-based analysis by Smith et al. (2022), much of the area where high confidence water occurs in the Central Valley is on cultivated croplands. This pattern is also observed in the current study, with the most significant

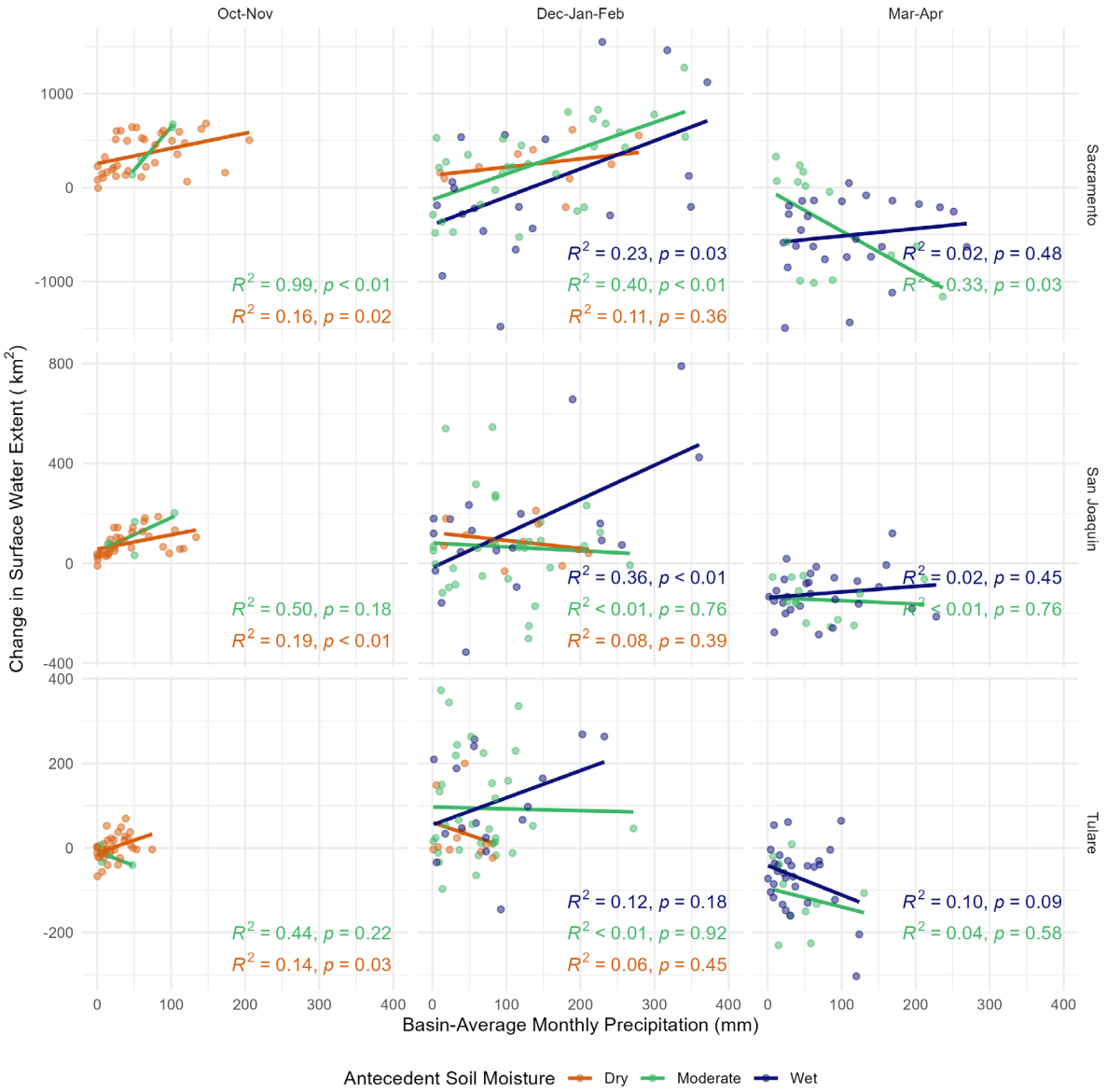

FIGURE 3 | Changes in surface water extents, as indicated by areal extents of DSWEmod High Confidence Water (HCW), by season, in relation to monthly precipitation and categories of antecedent soil moisture in the study area basins, 2003–2023. R^2 is based on the linear regression of DSWEmod HCW change and monthly basin-average precipitation (mm).

relationships between precipitation and water transitions occurring on this land cover type (refer to Figure S3). Places where significant relationships exist could indicate either intentional flooding for cropland management or unintentional flooding, and this could vary depending on the time of year and the underlying crop type (Smith et al. 2022). Intersecting statistically significant pixels with point data from the National Structure Inventory (NSI) and National Flood Insurance Program (NFIP) claims data highlights differences in exposure among areas with differing flood designation status (Figure 7). Based on the overlay of statistically significant pixels with NSI point data, the greatest exposure of structures (excluding contents and vehicles) actually occurs within Minimal Flood Hazard areas, with residential structures having the most value exposed. Similarly, nearly 60% ($22.5 million) of NFIP damage claims in the study area occurred in areas where minimal flood risk was the dominant flood designation (Figure 7). Although insurance claim damages are only a fraction of total value exposed, the NFIP data corroborate the potentially greater exposure observed in areas outside the 100- and 500-year flood boundaries.

4.4 | Relation of Precipitation-Driven Surface Water Appearances to Managed Aquifer Recharge Potential

We overlaid our results with an aquifer recharge suitability dataset, the Soil Agricultural Groundwater Banking Index (SAGBI; O'Geen et al. 2015) to assess the degree of overlap between precipitation-driven surface water occurrences and natural infrastructure (Figure 8). Of the 1800 km^2 area with significant relationships between precipitation and surface water transitions, 86% (unmodified) and 75% (modified) are classified as having poor to very poor recharge potential. Most of this area is within 5–10 km of Moderately Good or Good recharge potential lands, which offer opportunities to route water over short distances to

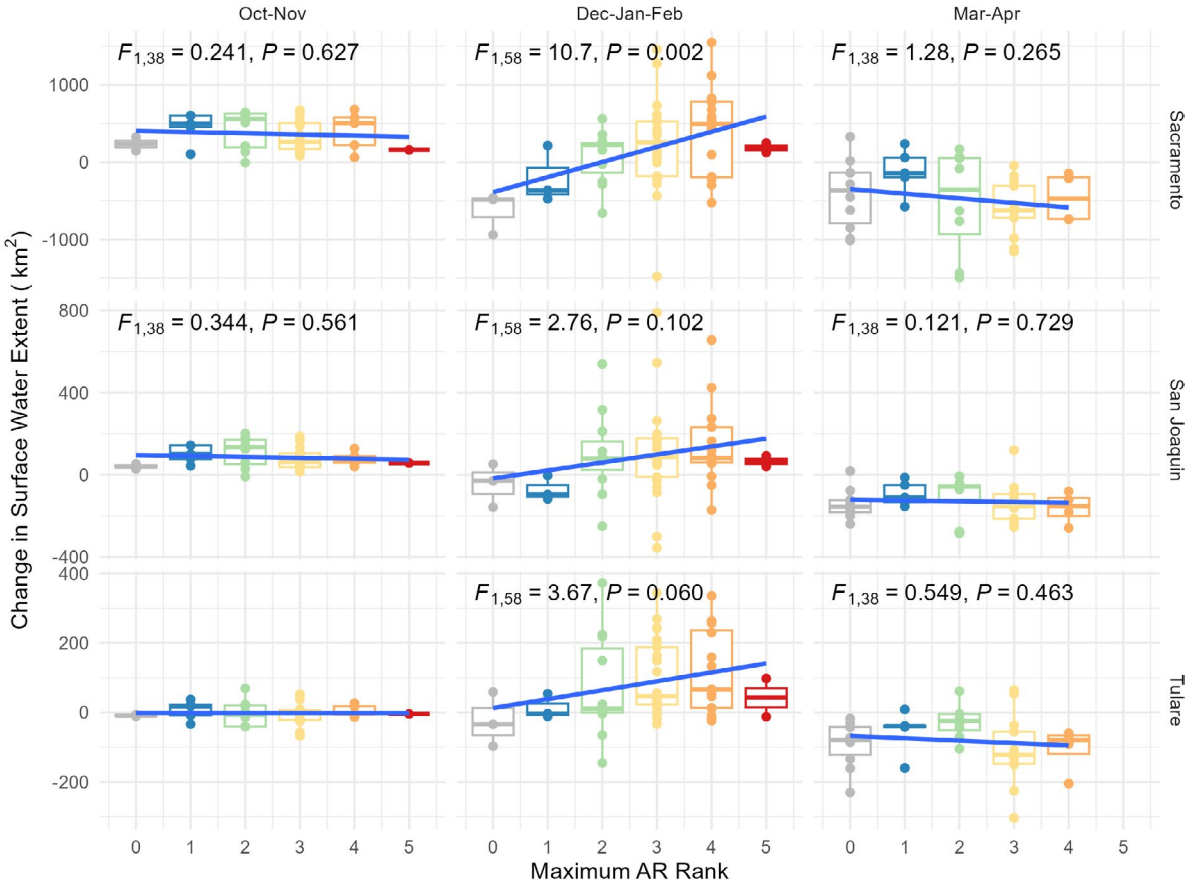

FIGURE 4 | Monthly changes in surface water extents, as indicated by DSWEmod High Confidence Water (HCW) area within the Sacramento, San Joaquin, and Tulare basins in relation to the maximum Atmospheric River (AR) rank in autumn ($n = 40$), winter ($n = 60$), and spring ($n = 40$). Data are derived from all monthly summaries of DSWEmod HCW change and AR events from 2003 through 2023. *F*- and *p*-values are based on differences in HCW area among monthly maximum AR ranks. Although not shown, results are similar when using the monthly sum of AR water vapor transport.

increase recharge potential, though proximities to Excellent recharge potential lands are generally longer distances.

5 | Discussion

5.1 | Basin Scale Analysis of Surface Water Extents Provides New Understanding of Mid-Winter Surface Water Dynamics

Overall, our basin-scale results highlight the co-dominant influences of precipitation variability, water conveyance, and cropland water management as drivers of surface water extents across the region at different times of year. For example, aside from a handful of large storm events occurring in mid-winter under wet antecedent soil moisture conditions that resulted in the largest increases in surface water extents, most large increases in surface water extents in the Sacramento and San Joaquin Valleys occur during October–November (Figures 2 and 5), when precipitation amounts tend to be smaller and antecedent soil moisture conditions are typically dry. These increases are independent of climate effects; instead, the increases are driven by the post-harvest agricultural practice of flooding rice fields to increase decomposition of crop residue and simultaneously support shorebird migration (Reiter et al. 2015). Springtime declines in surface water extents are also partially controlled by agricultural management (Schaffer-Smith et al. 2017), though extents tend to stay larger later in the season in wetter years (Figure 2) due to snowmelt. The patterns of surface water extent changes in autumn and early spring presented here are generally consistent with past Landsat-based studies in the Central Valley that focused on July–December (Reiter et al. 2015) and February–May (Schaffer-Smith et al. 2017), suggesting that Landsat data timeseries could be used for assessing historical variation of surface water outside of the winter season, because of its longer timeseries and finer spatial resolution. The omission of winter months in these previous Landsat-based studies highlights the important gap that DSWEmod fills in terms of understanding surface water dynamics in mid-winter, when precipitation is greatest, surface water extents are largest (Figure 2) and relationships between the two are strongest (Figure 4).

5.2 | Pixel Scale Analysis of Surface Water Changes Highlights Locations of High-Frequency Precipitation-Driven Flooding

The pixel scale analysis highlights locations where surface water appears in response to precipitation at relatively high monthly frequency, providing insights into infrastructure and

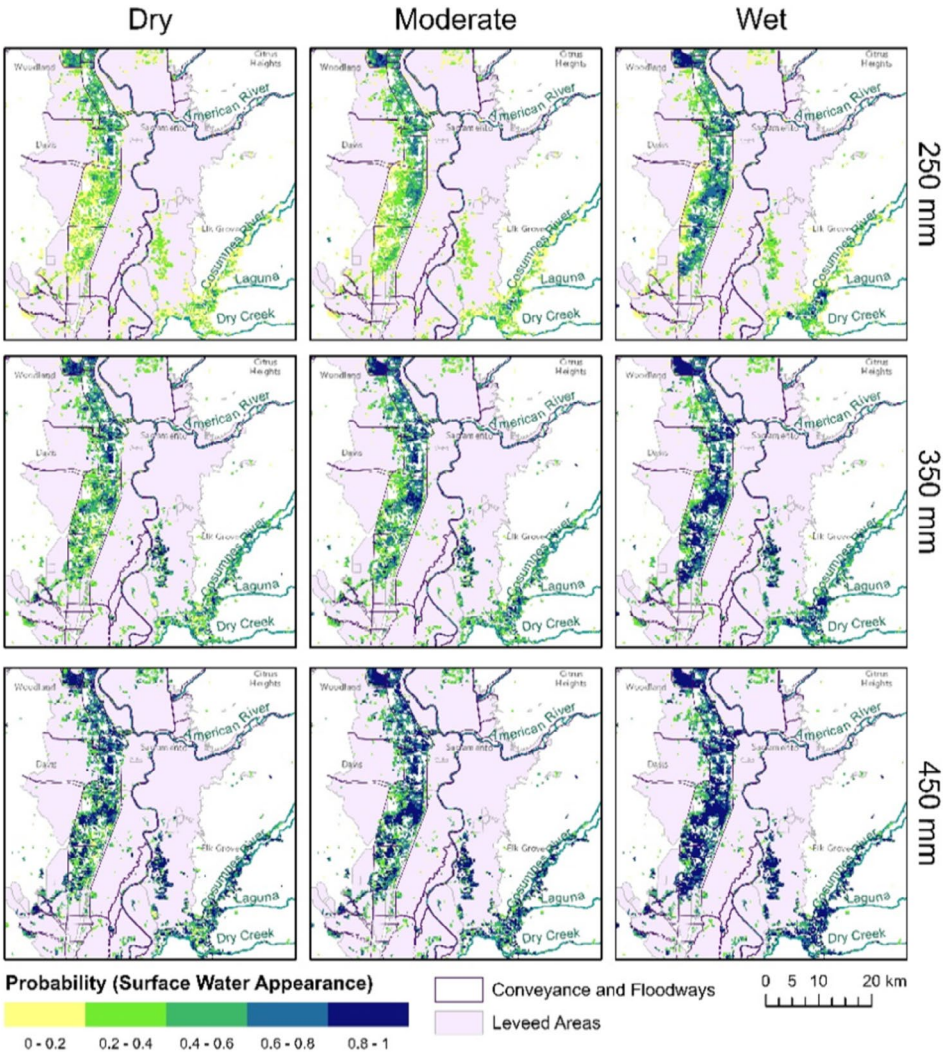

FIGURE 5 | Predicted probabilities of surface water appearance at 250, 350, and 450 mm HUC 4 spatially averaged monthly precipitation under dry, moderate, and wet antecedent soil moisture conditions in the lower Sacramento basin. Only pixel values with statistically significant relations to precipitation ($p < 0.10$) are shown. Purple lines indicate conveyance and floodway routes. Data can be further explored using the map application: http://dri-apps.projects.earthengine.app/view/dsweprobabilities.

community exposures and vulnerabilities that may be less well recognized relative to those that occur during the largest floods (Selsor et al. 2023). Overall, water largely follows expected pathways along rivers, conveyance channels, and floodways, with increasing probabilities of occurrence as precipitation amounts and antecedent soil moisture increase. Yet, there are several areas both within and outside of designated flood boundaries and leveed areas that have statistically significant precipitation-driven surface water occurrences, highlighting locations that may merit additional study and consideration in flood planning. Results from this study could also provide calibration and/or validation data for higher spatial resolution hydrologic and hydraulic models (e.g., HEC-HMS and HEC-RAS) that are used for flood risk management studies (Di Baldassarre et al. 2009) and flood managed aquifer recharge feasibility studies. Models are typically used in flood risk management studies to demarcate anticipated inundation extents within large population centers and for the largest flood events. DSWEmod results could supplement these hi-resolution models by providing estimates of inundation extents that occur more frequently or outside of large population centers, which can help to inform decisions about future development and/or management of these areas, including the potential for flood risk reduction via flood managed aquifer recharge projects.

We note that these results do not necessarily reflect probabilities of exposure to large flood events for several reasons. Because the study period is limited to 2003–2023, the rarity of surface water occurrences corresponding to the largest flood events effectively precludes meeting criteria for statistical significance in our model due to the small sample size. For example, the study period does not capture several severe floods in the contemporary record (e.g., 1955, 1986, 1997) nor those in the more distant historic (e.g., 1862; Engstrom 1996) or paleoclimate records, which represent a much broader range of possibilities (Harden et al. 2021; Knight et al. 2024). The substantially larger confidence intervals observed at higher precipitation amounts are another consequence of this small sample size. We also note that the use of monthly surface water transitions as the response variable limits our inferences to those locations where surface

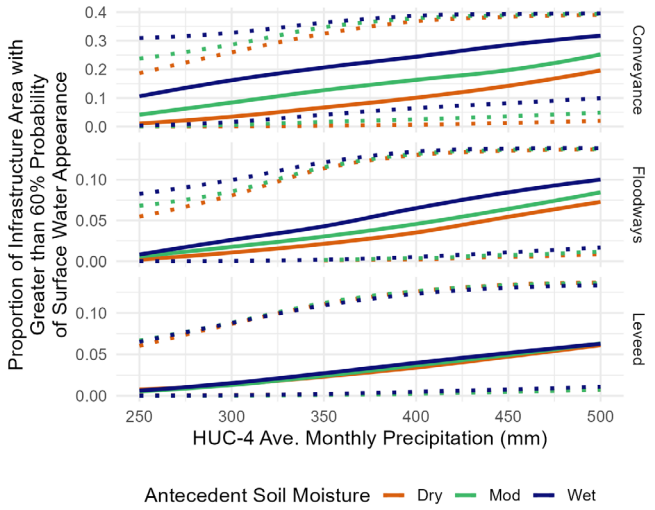

FIGURE 6 | Proportion of conveyance, floodway, and leveed areas in the Sacramento portion of the Central Valley with greater than 60% probabilities of surface water appearances across monthly precipitation amounts and under dry, moderate, and wet antecedent conditions. Solid lines indicate predicted values; dotted lines indicate values at upper and lower confidence limits. Larger precipitation amounts result in increased probabilities over larger areas in all infrastructure types. Wetter antecedent soil moisture enhances probabilities in conveyance channels and has little influence in leveed areas.

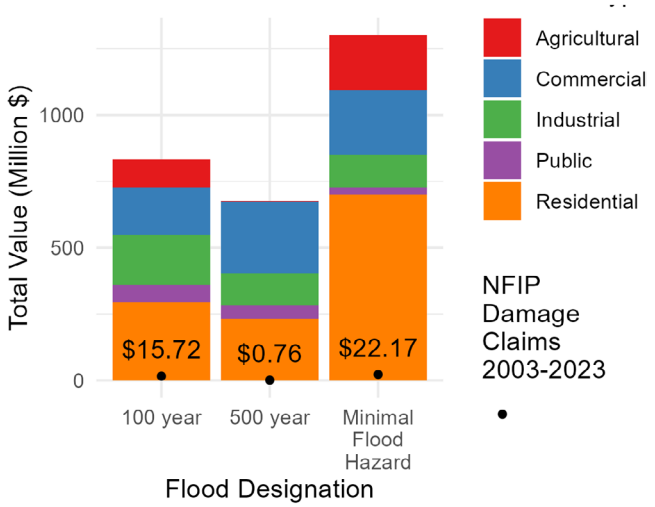

FIGURE 7 | Total value of structures from the National Structure Inventory by occupancy type, occurring within pixels with statistically significant ($p < 0.10$) transitions to water and classified by highest flood risk designation based on the composite of CADWR, USACE, and DFIRM flood boundaries. Total claimed residential damages (2003–2023) through the National Flood Insurance Program (NFIP) are shown as points within each flood designation. Maps showing NFIP damages, exposed NSI structures, and composite flood boundaries in select areas are shown in Figure S4. Locations of statistically significant transitions to water relative to 100- and 500- year flood boundaries can be viewed interactively at https://dri-apps.projects.earthengine.app/view/dsweprobabilities.

water occurrences relate to precipitation occurring in the same month, which likely excludes instances where flood responses are delayed due to reservoir storage or precipitation occurring as snow. This may partly explain the lack of statistically significant results in the San Joaquin and Tulare, where the proportions of precipitation occurring as snow are larger than in the Sacramento (Lund 2012). Because our study period ended in January 2023, we did not capture the extensive flooding that occurred in the Tulare in late spring 2023. The larger uncertainties associated with rarer events are especially important to consider in the context of using these results to understand future flood risks. While increases in storm intensities and decreases in the snow to rain ratio are likely to result in increases in probabilities of transitions to water in places identified in our results, probabilities are not shown for places that did not meet statistical significance criteria. Areas that lack statistical significance still have the potential to be affected by the rarer and largest floods. This possibility is especially acute in the San Joaquin and Tulare basins, where snow-to-rain transitions under future climate are likely to cause more immediate responses that were likely not detected here given the analytical approach, which focused on flood responses occurring in the same month as precipitation.

5.3 | Structural Exposure to Flooding Is High Outside of 100- and 500-Year Flood Boundaries

Overlays of statistically significant pixels with the National Structure Inventory (NSI) indicate that the most exposure, in terms of structure values, is associated with residential structures, and that there is greater value exposed outside of 100- and 500-year flood boundaries than within. This pattern is also observed in National Flood Insurance Program (NFIP) claims data. Whether this exposure is due to inadequacies in flood risk assessments or simply demonstrates the success of concentrating development outside of flood zones is not clear. Additional study focused on the age of exposed infrastructure and trends in development could provide further insights into this pattern.

Locations with NFIP claims greater than $1 million include areas along the Sacramento River near Red Bluff, the American River in Sacramento, Dry Creek in Roseville (North Sacramento), Butte Creek (south of Chico), the Consumnes River near Wilton, and the San Joaquin River near Antioch (Figure S4). Of these, exposures of structures are observed along the Sacramento, Feather, American, and Consumnes Rivers, but not along smaller-sized creeks, where DSWEmod is too spatially coarse to capture flood occurrences. Structural exposures were also not observed along the San Joaquin River near Antioch, which may be due to low confidence in water detections due to urban land cover adjacent to the San Joaquin River.

The number of pixels with statistical significance results in a conservative estimate of locations with precipitation-driven inundation given our choice to include only the highest confidence water detections in our analysis, and our subsequent filtering step, which excluded isolated areas where precipitation-driven surface water appearances were detected. Despite this, the number of structures with inundation exposure could still be overestimated, given that any structure falling within the 250-m MODIS pixel is assumed to be exposed. We elected to use MODIS for our winter-season focused study because longer timeseries are needed to discern anomalous surface water extents that constitute flooding from those that represent typical variability, given

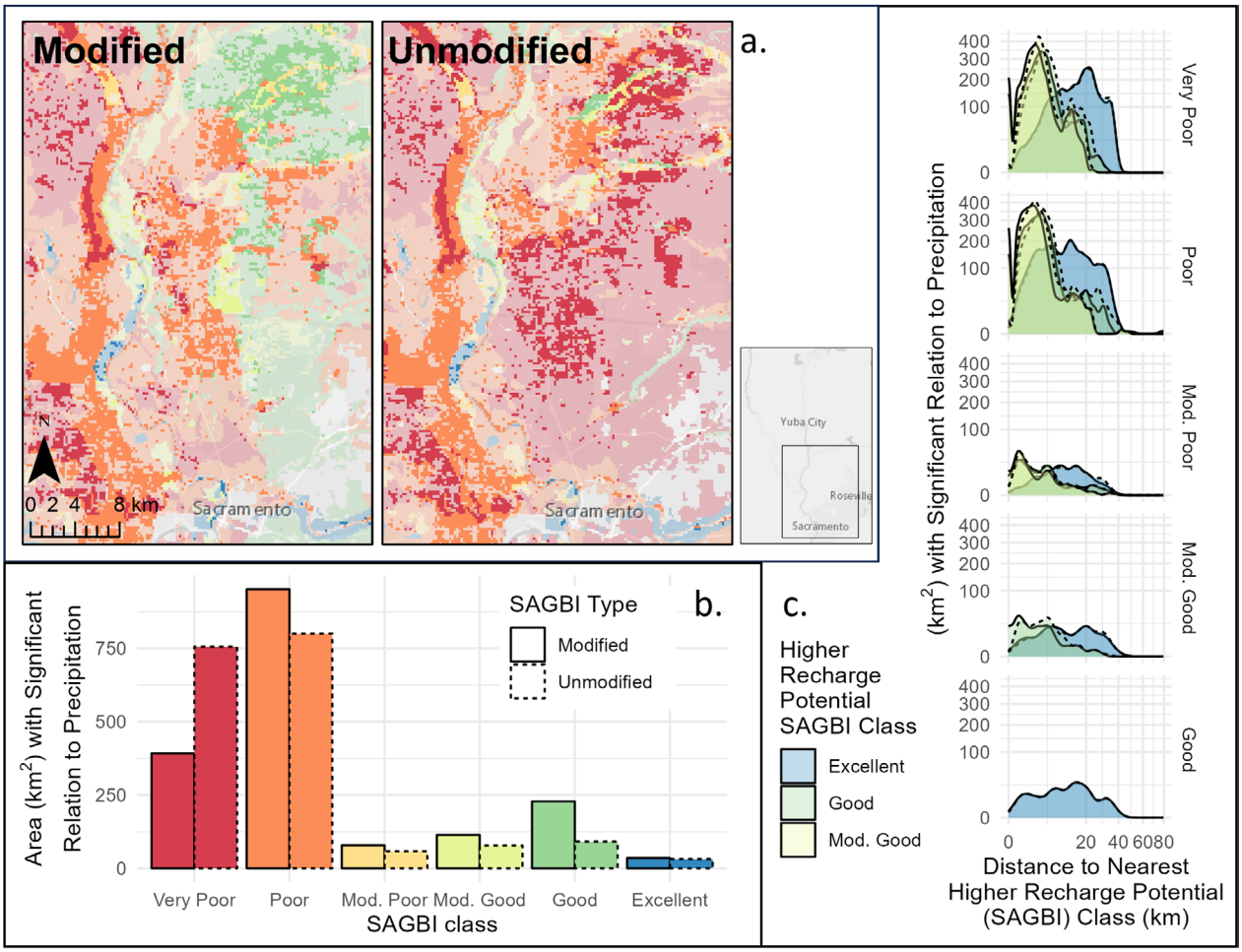

FIGURE 8 | (a) Map showing modified and unmodified Soil Agricultural Groundwater Banking Index (SAGBI) classes for an example area in the Lower Sacramento basin. Modified SAGBI represents theoretical recharge suitability, assuming soils with restrictive layers have been deep tilled to improve recharge potential. Areas without statistically significant relations ($p < 0.10$) to precipitation are indicated as semi-transparent colors. (b) Areal extents of pixels with statistically significant relations to precipitation across SAGBI classes within the entire study area. (c) Minimum distances from statistically significant pixels in a given SAGBI (very poor to good) class to those with higher recharge potential (Moderately Good, Good, Excellent SAGBI classes) within the entire study area.

the season (Brakenridge 2018). As timeseries grow for platforms such as Sentinel-1 C-band synthetic aperture radar (SAR), which has 10-m spatial resolution, quasi-weekly temporal resolution, and cloud penetrations, more accurate numbers can likely be derived in future studies.

5.4 | Precipitation-Driven Flooding Occurs in Areas With Low Managed Aquifer Recharge Potential

The more widespread occurrence of surface water in soil types with very poor to poor suitability for managed aquifer recharge could be due to multiple factors. Fundamentally, the odds of detecting standing water through remote sensing are higher in places where soil hydraulic conductivities are low and infiltration rates are slow, whereas in places with better recharge potential, surface water occurrences may be missed due to more immediate infiltration. Additionally, these results reflect the inherent distributions of uniformly fine-textured soils that are less ideal for flood managed aquifer recharge and natural runoff accumulation within the study area. Regardless, results presented here have the potential to inform managed aquifer recharge planning in multiple ways. First, this study identifies where flood waters naturally or commonly occur during the non-growing season, when water availability is high and recharge opportunities are likely the greatest. Although recharge is typically slow in these poor recharge potential areas, the large extent and persistence of surface water in these landscapes could yield a significant volume of water to aquifers, especially if interventions were targeted to increase infiltration capacities in these places or convey water to more suitable soils for aquifer recharge. Second, identifying locations with high probability of inundation near areas with high recharge potential may support groundwater planning under California's Sustainable Groundwater Management Act (State of California 2014) and the Multibenefit Land Repurposing Program (California Department of Conservation 2021). This planning may involve prioritizing agricultural areas for fallowing or transitioning from permanent to annual crops, which are better suited to the prolonged saturation of flood managed aquifer recharge on agricultural lands (Ganot and Dahlke 2021). Additionally,

understanding where probabilities of inundation are high can guide regional decisions on the development, maintenance, or operation of conveyance infrastructure to connect areas of high surface water occurrence with nearby soil landscapes that are more suitable for recharge. Moreover, understanding the relationship of surface water transitions with basin precipitation can enable the use of weather forecasts to guide preparations and decision-making related to flood risk mitigation and enhancing water supplies through targeted aquifer recharge activities. Finally, although some regulatory challenges must still be overcome to enable recharge from flood events (Kocis and Dahlke 2017), progress has been made over the past several years, including the most recent California Senate Bill 122 (July 2024), which revised California Water Code (Section 1242.1) to enable diversion of flood waters without water rights under certain circumstances.

6 | Conclusions

Our study utilizes 20 years of MODIS satellite imagery to map surface water dynamics across California's Central Valley, which provides critical information of surface water extents and associated flood risk in response to precipitation events. Our results demonstrated the utility of the daily DSWEmod product for deriving continuous timeseries of mapped surface water extents, during seasons with high incidence of cloud cover, which is a limitation of other long-term optical satellite remote sensing data due to their lower temporal frequency. The resulting product was used to analyze relationships between inundation occurrence and climatic driving forces across the predominantly agricultural and moderately urbanized landscape of the Central Valley. Our results provide a greater understanding of the dynamics and driving forces of surface water inundation patterns. This is consequential for optimizing diverse land use planning and management activities, including agricultural crop practices, infrastructure and urban development, and groundwater recharge. Our findings also highlight where precipitation-driven surface water appearances most commonly deviate outside of designated (e.g., FEMA, USACE) flood boundaries, a result that is further supported by National Flood Insurance Program claims data. The greater value of structures exposed outside of designated flood boundaries highlight the need for improved flood mapping, awareness, and mitigation. Additionally, our results provide an opportunity for floodwater management planning to reduce flood risk in areas with higher frequencies of surface water inundation and consider managed aquifer recharge potentials to mitigate this risk. This could be achieved by identifying locations where land restoration or floodwater routing offer the greatest opportunities for increasing groundwater recharge and associated regional multibenefits. Finally, our study shows the potential for the daily DSWEmod product to be used as a novel decision-support tool, because it provides critical information of where actual observable surface water extent frequencies are occurring in contemporary times despite cloud cover limitations faced when using other satellite-based products. Cloud cover issues are common during high precipitation (wet season) periods and surface water extents are most consequential in terms of both flood risks and water supplies. Thus, the approach described here is not only applicable in California's Central Valley; it can also be applied in other regions where the observation of wet-season surface water dynamics can support flood management decisions.

Results from this study are readily visualized and available within three web applications, including (1) monthly timeseries of both Landsat and MODIS DSWE over their periods of record, which can be used to view specific events: https://dri-apps.projects.earthengine.app/view/dswe, (2) monthly frequencies of DSWEmod, which can be used to view and export timeseries of DSWEmod and monthly climate for specific pixels: https://dri-apps.projects.earthengine.app/view/dswemodmonthlyfreq, and (3) predicted probabilities (with uncertainty ranges) of surface water appearances under different precipitation and antecedent soil moisture conditions, based on our model results: https://dri-apps.projects.earthengine.app/view/dsweprobabilities.

Acknowledgments

Funding for this work was provided by the US Geological Survey through grant agreement number G21AC10098 and the US Army Corps of Engineers, Engineer Research and Development Center through grant agreement number W912HZ1920011. The authors wish to thank Natasha Wesely for assistance with compiling watershed data for this study, as well as Michael Meyers (USGS) and two anonymous reviewers for their suggestions that helped to improve this manuscript. Any use of trade, firm, or product names is for descriptive purposes only and does not imply endorsement by the US Government.

Data Availability Statement

The data that support the findings of this study are available from the corresponding author upon reasonable request.

References

Albano, C. M., C. E. Soulard, B. A. Minor, J. J. Walker, B. W. Smith, and E. K. Waller. 2025. "Data on Winter Surface Water Dynamics in California's Central Valley Using Satellite Remote Sensing (Csv, xml)." US Geological Survey. https://doi.org/10.5066/P1KJLAMN.

Bates, D., M. Mächler, B. Bolker, and S. Walker. 2015. "Fitting Linear Mixed-Effects Models Using lme4." *Journal of Statistical Software* 67, no. 1: 1–48. https://doi.org/10.18637/jss.v067.i01.

Brakenridge, G. R. 2018. "Flood Risk Mapping From Orbital Remote Sensing." In *Geophysical Monograph Series*, edited by G. J.-P. Schumann, P. D. Bates, H. Apel, and G. T. Aronica, 43–54. John Wiley & Sons, Inc. https://doi.org/10.1002/9781119217886.ch3.

California Department of Conservation. 2021. "Multibenefit Land Repurposing Program (MLRP)." https://www.conservation.ca.gov/dlrp/grant-programs/Pages/Multibenefit-Land-Repurposing-Program.aspx.

California Department of Water Resources. 2022. "Central Valley Flood Protection Plan Update 2022." State of California Natural Resources Agency. https://water.ca.gov/-/media/DWR-Website/Web-Pages/Programs/Flood-Management/Flood-Planning-and-Studies/Central-Valley-Flood-Protection-Plan/Files/CVFPP-Updates/2022/Central_Valley_Flood_Protection_Plan_Update_2022_ADOPTED.pdf.

Cao, Q., A. Gershunov, T. Shulgina, F. M. Ralph, N. Sun, and D. P. Lettenmaier. 2020. "Floods due to Atmospheric Rivers Along the US West Coast: The Role of Antecedent Soil Moisture in a Warming Climate." *Journal of Hydrometeorology* 21, no. 8: 1827–1845. https://doi.org/10.1175/JHM-D-19-0242.1.

Charles, D. 2023. "Can California's Floods Help Recharge Depleted Aquifers?" *Science* 379, no. 6630: 320–322. https://doi.org/10.1126/science.adg8345.

Corringham, T. W., and D. R. Cayan. 2019. "The Effect of El Niño on Flood Damages in the Western United States." *Weather, Climate, and Society* 11, no. 3: 489–504. https://doi.org/10.1175/WCAS-D-18-0071.1.

Corringham, T. W., F. M. Ralph, A. Gershunov, D. R. Cayan, and C. A. Talbot. 2019. "Atmospheric Rivers Drive Flood Damages in the Western United States." *Science Advances* 5, no. 12: eaax4631. https://doi.org/10.1126/sciadv.aax4631.

Dettinger, M., D. Lavers, J. Rutz, M. Viale, A. Wade, and A. B. White. 2019. "Effects of Atmospheric Rivers." In *Atmospheric Rivers*, edited by F. M. Ralph, M. D. Dettinger, D. E. Waliser, and J. J. Rutz, 40. Springer International.

Di Baldassarre, G., G. Schumann, and P. D. Bates. 2009. "A Technique for the Calibration of Hydraulic Models Using Uncertain Satellite Observations of Flood Extent." *Journal of Hydrology* 367, no. 3: 276–282. https://doi.org/10.1016/j.jhydrol.2009.01.020.

Engstrom, W. N. 1996. "The California Storm of January 1862." *Quaternary Research* 46, no. 2: 141–148. https://doi.org/10.1006/qres.1996.0054.

Erlingis, J. M., M. Rodell, C. D. Peters-Lidard, et al. 2021. "A High-Resolution Land Data Assimilation System Optimized for the Western United States." *Journal of the American Water Resources Association* 57, no. 5: 692–710. https://doi.org/10.1111/1752-1688.12910.

Faunt, C. C., M. Sneed, J. Traum, and J. T. Brandt. 2016. "Water Availability and Land Subsidence in the Central Valley, California, USA." *Hydrogeology Journal* 24, no. 3: 675–684. https://doi.org/10.1007/s10040-015-1339-x.

Federal Emergency Management Agency. 2024. "OpenFEMA Dataset: FIMA NFIP Redacted Claims—V2 (Version 2)." https://www.fema.gov/openfema-data-page/fima-nfip-redacted-claims-v2#.

Ganot, Y., and H. E. Dahlke. 2021. "A Model for Estimating ag-MAR Flooding Duration Based on Crop Tolerance, Root Depth, and Soil Texture Data." *Agricultural Water Management* 255: 107031. https://doi.org/10.1016/j.agwat.2021.107031.

Gershunov, A., T. Shulgina, F. M. Ralph, D. A. Lavers, and J. J. Rutz. 2017. "Assessing the Climate-Scale Variability of Atmospheric Rivers Affecting Western North America." *Geophysical Research Letters* 44, no. 15: 7900–7908. https://doi.org/10.1002/2017GL074175.

Gorelick, N., M. Hancher, M. Dixon, S. Ilyushchenko, D. Thau, and R. Moore. 2017. "Google Earth Engine: Planetary-Scale Geospatial Analysis for Everyone." *Remote Sensing of Environment* 202: 18–27. https://doi.org/10.1016/j.rse.2017.06.031.

Harden, T., K. Ryberg, J. O'Connor, J. Friedman, and J. Kiang. 2021. "Historical and Paleoflood Analyses for Probabilistic FloodHazard Assessments—Approaches and Review Guidelines (US Geological Survey Techniques and Methods 4-B6; Techniques and Methods)."

Heimhuber, V., M. G. Tulbure, and M. Broich. 2017. "Modeling Multidecadal Surface Water Inundation Dynamics and Key Drivers on Large River Basin Scale Using Multiple Time Series of E Arth-Observation and River Flow Data." *Water Resources Research* 53, no. 2: 1251–1269. https://doi.org/10.1002/2016WR019858.

Jones, J. 2019. "Improved Automated Detection of Subpixel-Scale Inundation—Revised Dynamic Surface Water Extent (DSWE) Partial Surface Water Tests." *Remote Sensing* 11, no. 4: 374. https://doi.org/10.3390/rs11040374.

Knight, C. A., L. Anderson, L. Presnetsova, M. Champagne, and D. Wahl. 2024. "Atmospheric River Activity During the Late Holocene Exceeds Modern Range of Variability in California." *Communications Earth & Environment* 5, no. 1: 216. https://doi.org/10.1038/s43247-024-01357-z.

Knowles, J. E., and C. Frederick. 2020. "merTools: Tools for Analyzing Mixed Effect Regression Models." https://CRAN.R-project.org/package=merTools.

Kocis, T. N., and H. E. Dahlke. 2017. "Availability of High-Magnitude Streamflow for Groundwater Banking in the Central Valley, California." *Environmental Research Letters* 12, no. 8: 084009. https://doi.org/10.1088/1748-9326/aa7b1b.

Lüdecke, D., M. Ben-Shachar, I. Patil, P. Waggoner, and D. Makowski. 2021. "Performance: An R Package for Assessment, Comparison and Testing of Statistical Models." *Journal of Open Source Software* 6, no. 60: 3139. https://doi.org/10.21105/joss.03139.

Lund, J. R. 2012. "Flood Management in California." *Water* 4, no. 1: 157–169. https://doi.org/10.3390/w4010157.

O'Geen, A. T., M. Saal, H. Dahlke, et al. 2015. "Soil Suitability Index Identifies Potential Areas for Groundwater Banking on Agricultural Lands." *California Agriculture* 69, no. 2: 75–84. https://doi.org/10.3733/ca.v069n02p75.

Pekel, J.-F., A. Cottam, N. Gorelick, and A. S. Belward. 2016. "High-Resolution Mapping of Global Surface Water and Its Long-Term Changes." *Nature* 540, no. 7633: 418–422. https://doi.org/10.1038/nature20584.

Policelli, F., D. Slayback, B. Brakenridge, et al. 2017. "The NASA Global Flood Mapping System." In *Remote Sensing of Hydrological Extremes*, edited by V. Lakshmi, 47–63. Springer International Publishing. https://doi.org/10.1007/978-3-319-43744-6_3.

R Core Team. 2024. "R: A Language and Environment for Statistical Computing [Computer Software]." R Foundation for Statistical Computing. https://www.R-project.org/.

Ralph, F. M., T. Coleman, P. J. Neiman, R. J. Zamora, and M. D. Dettinger. 2013. "Observed Impacts of Duration and Seasonality of Atmospheric-River Landfalls on Soil Moisture and Runoff in Coastal Northern California." *Journal of Hydrometeorology* 14, no. 2: 443–459. https://doi.org/10.1175/JHM-D-12-076.1.

Ralph, F. M., M. D. Dettinger, J. J. Rutz, and D. E. Waliser, eds. 2020. *Atmospheric Rivers*. Springer International Publishing. https://doi.org/10.1007/978-3-030-28906-5.

Ralph, F. M., J. J. Rutz, J. M. Cordeira, et al. 2019. "A Scale to Characterize the Strength and Impacts of Atmospheric Rivers." *Bulletin of the American Meteorological Society* 100, no. 2: 269–289. https://doi.org/10.1175/BAMS-D-18-0023.1.

Reddy, V. R., P. Pavelic, and M. A. Hanjra. 2017. "Underground Taming of Floods for Irrigation (UTFI) in the River Basins of South Asia: Institutionalising Approaches and Policies for Sustainable Water Management and Livelihood Enhancement." *Water Policy* 20, no. 2: 369–387. https://doi.org/10.2166/wp.2017.150.

Reiter, M. E., N. Elliott, S. Veloz, et al. 2015. "Spatio-Temporal Patterns of Open Surface Water in the Central Valley of California 2000-2011: Drought, Land Cover, and Waterbirds." *Journal of the American Water Resources Association* 51, no. 6: 1722–1738. https://doi.org/10.1111/1752-1688.12353.

Schaffer-Smith, D., J. J. Swenson, B. Barbaree, and M. E. Reiter. 2017. "Three Decades of Landsat-Derived Spring Surface Water Dynamics in an Agricultural Wetland Mosaic; Implications for Migratory Shorebirds." *Remote Sensing of Environment* 193: 180–192. https://doi.org/10.1016/j.rse.2017.02.016.

Selsor, H., B. P. Bledsoe, and R. Lammers. 2023. "Recognizing Flood Exposure Inequities Across Flood Frequencies." *Anthropocene* 42: 100371. https://doi.org/10.1016/j.ancene.2023.100371.

Smith, B. W., C. E. Soulard, J. J. Walker, and A. M. Wein. 2022. "Using Landsat and MODIS Satellite Collections to Examine Extent, Timing, and Potential Impacts of Surface Water Inundation in California Croplands." *Remote Sensing Applications: Society and Environment* 28: 100837. https://doi.org/10.1016/j.rsase.2022.100837.

Soulard, C. E., E. K. Waller, J. J. Walker, and R. E. Petrakis. 2021. "DSWEmod Surface Water Map Composites Generated From Daily MODIS Images—California." https://doi.org/10.5066/P9RVPJWE.

Soulard, C. E., E. K. Waller, J. J. Walker, R. E. Petrakis, and B. W. Smith. 2022. "DSWEmod—The Production of High-Frequency Surface Water Map Composites From Daily MODIS Images." *JAWRA Journal of the American Water Resources Association* 58, no. 2: 248–268. https://doi.org/10.1111/1752-1688.12996.

State of California. 2014. "Sustainable Groundwater Management Act." https://leginfo.legislature.ca.gov/faces/codes_displayexpandedbranch.xhtml?tocCode=WAT&division=6.&title=&part=2.74.&chapter=&article.

Sumargo, E., H. McMillan, R. Weihs, C. J. Ellis, A. M. Wilson, and F. M. Ralph. 2021. "A Soil Moisture Monitoring Network to Assess Controls on Runoff Generation During Atmospheric River Events." *Hydrological Processes* 35, no. 1: e13998. https://doi.org/10.1002/hyp.13998.

Tellman, B., J. A. Sullivan, C. Kuhn, et al. 2021. "Satellite Imaging Reveals Increased Proportion of Population Exposed to Floods." *Nature* 596: 7870. https://doi.org/10.1038/s41586-021-03695-w.

Tjur, T. 2009. "Coefficients of Determination in Logistic Regression Models – A New Proposal: The Coefficient of Discrimination." *American Statistician* 63, no. 4: 366–372. https://doi.org/10.1198/tast.2009.08210.

US Army Corps of Engineers. 2019. "National Structure Inventory (NSI) Base Data." https://www.hec.usace.army.mil/confluence/nsi/technicalreferences/2019.

US Census Bureau. 2022. "TIGER/Line Shapefiles, Roads." https://www.census.gov/cgi-bin/geo/shapefiles/index.php.

US Geological Survey. 2019. "US Geological Survey, 2019, National Hydrography Dataset ver. USGS National Hydrography Dataset Best Resolution (NHD) for Hydrologic Unit (HU) 4." https://www.usgs.gov/national-hydrography/access-national-hydrography-products.

Vanderhoof, M. K., J. Christensen, Y.-J. G. Beal, et al. 2020. "Isolating Anthropogenic Wetland Loss by Concurrently Tracking Inundation and Land Cover Disturbance Across the Mid-Atlantic Region, U.S." *Remote Sensing* 12, no. 9: 1464. https://doi.org/10.3390/rs12091464.

Vuolo, F., W.-T. Ng, and C. Atzberger. 2017. "Smoothing and Gap-Filling of High Resolution Multi-Spectral Time Series: Example of Landsat Data." *International Journal of Applied Earth Observation and Geoinformation* 57: 202–213. https://doi.org/10.1016/j.jag.2016.12.012.

Walker, J. J., C. E. Soulard, and R. E. Petrakis. 2020. "Integrating Stream Gage Data and Landsat Imagery to Complete Time-Series of Surface Water Extents in Central Valley, California." *International Journal of Applied Earth Observation and Geoinformation* 84: 101973. https://doi.org/10.1016/j.jag.2019.101973.

Wooldridge, J. M. 2012. *Introductory Econometrics: A Modern Approach*. 5th ed. South Western Cengage Learning.

Wulder, M. A., J. C. White, T. R. Loveland, et al. 2016. "The Global Landsat Archive: Status, Consolidation, and Direction." *Remote Sensing of Environment* 185: 271–283. https://doi.org/10.1016/j.rse.2015.11.032.

Zhu, Y., and R. E. Newell. 1998. "A Proposed Algorithm for Moisture Fluxes From Atmospheric Rivers." *Monthly Weather Review* 126, no. 3: 725–735. https://doi.org/10.1175/1520-0493(1998)126<0725:APAFMF>2.0.CO;2.

Supporting Information

Additional supporting information can be found online in the Supporting Information section.